Heavy Charged-Particle Beam Dosimetry

LBL--14779

DE82 020315

John T. Lyman, Ph.D
Lawrence Berkeley Laboratory
University of California
Berkeley, CA 94720
USA

IAEA Advisory Group Meeting
Advances in Dosimetry for Fast Neutrons
and
Heavy Charged-Particles
for Therapy Applications

Vienna Austria
June 14-18, 1982

This work was supported by the U.S. Department of Energy under
Contract Number DE-AC03-76SF00098.

Heavy Charged-Particle Beam Dosimetry

Abstract

A computational description of the physical properties and the beam composition of a heavy charged-particle beam is presented. The results with this beam model has been compared with numerous sets of experimental data and it appears to provide an adequate representation of the major features of a heavy charged-particle beam. Knowledge of the beam compositon aids in the identification of regions of the beam where special dosimetry problems may be encountered.

1. Introduction

For heavy charged particles, the absorbed dose can be determined from a knowledge of the charged particle fluence spectrum ϕ and the stopping power S of the absorber material at the point of interest [1]. If the energy of the particles is denoted by E, and if delta ray equilibrium is established, the dose in a small mass inside a homogeneous medium is given by

$$D = \frac{1}{\rho}\int_0^{E_m} \phi\,(E)\; S\,(E)\; dE \qquad \text{Eq. 1.}$$

where E_m is the maximum kinetic energy of the particles and ρ is the density of the medium.

The knowledge of the charged particle fluence spectrum is a valuable aid to identifying the possible errors associated with the dosimetry. Both experimental and theoretical approaches are used to determine the beam composition and thereby identify the major contributors to the absorbed dose. Experimentally, beam properties are determined and particles are identified through the use of devices such as ionization chambers, Faraday cups, secondary emission monitors, plastic scintillators, silicon or germanium semiconductor detectors, calorimeters, thermoluminescent materials, nuclear emulsions and particle track detectors, [2-8]. Theoretical and empirical studies of the range-energy relationships, multiple scattering and fragmentation aid in the development of the computational beam model [9,10] which can be used to assist in interpretation and to supplement the available beam composition data.

2. Methods and Materials

The heavy charged-particle beams that have received the most interest in the biomedical program at Berkeley are the beams of helium, carbon, neon, silicon and argon ions. The energies and ranges in water of these beams varies from initial energies between 225 and 900 MeV/u and residual ranges between 3 and 30 cm.

Bragg curves of four different types of heavy particles beams (helium, carbon, neon, and argon) are shown in Figure 1. Two initial energies were used for each ion and the energy spread of beams is typically less than 0.5 percent. The Bragg curve is the average specific ionization as a function of penetration distance into an absorber. The differences in the shapes of the curves are due mainly to the probability of the primary ion being fragmented by a nuclear collision before it has completely given up its kinetic energy, and to the number and type of secondary particles produced.

The average energy of the primary ions at the Bragg peak depends upon the initial energy spread of the beam and the range straggling [10]. For protons, the average energy at the Bragg peak is typically about 10 percent of the initial energy [2] while for the heavier ions it is less because of the decrease in the range straggling of the heavier charged particles.

If the nuclear interactions are of a negligible importance, the Bragg curve can be obtained from the specific ionization of a single particle and the particle straggling distribution [11]. When nuclear interactions are important, the Bragg cruve is composed of the contributions of the primary ions and of the fragments which are produced by the nuclear interactions. The fragment contribution is composed of the ionization of the secondary particles and any of their fragments which may be produced by additional nuclear interactions. The probability for the loss of a primary particle depends on the size of the primary nucleus and the nuclei of the absorbing media [12]. The probability of producing a particular fragment is given by the empirical formulation of Silberberg and Tsao [13]. Based upon these principles, a beam model has been developed with which it is possible to predict many of the characteristics of a heavy charged-particle beam.

The Bragg peak is generally too narrow for most radiotherapy applications. To effectively utilize these beams for cancer therapy. The stopping region of the particles is modulated to produce a high-dose region broader than the Bragg peak, but still a region in which the biological effectiveness of the particles is greater than on either side of this region [10] (Fig. 2). This is accomplished by the superposition of Bragg peaks of beams with different ranges of penetration [5,14,15]. The positions of the least penetrating and most penetrating Bragg peaks are designated as the proximal and distal peaks and define the high dose region. If one understands the beams composition of a single Bragg curve, the more complicated dose distributions can also be understood if the distributions are separated into the individual Bragg curves.

3. Results

The beam model has been used to calculate many of the properties of a 557-MeV/u neon ion beam and some of the results are present in figures 3-11. As the primary ion loses energy to the absorbing medium, the kinetic energy decreases until the particle comes to rest (Fig. 3). The calculations of the range-energy and energy loss relations over this energy range are probably good to better than few percent [16] and curves of this type are easily verified by measurement.

The primary ions are either exponentially removed from the beam or lose all their kinetic energy and therefore come to rest (Fig. 4). The rate at which the ions are lost from the beam depends upon the ion mass. Lighter ions survive better than the heavier ions. The build-up of the secondary ions depends upon their rate of production and their rate of removal. The most numerous ions will be protons because they have the highest production probability, the lowest rate of loss.

The beam charge is the sum of the products of the number of each type of charged particle and its charge. This is a quantity that can be measured with a Faraday cup. If the charge carried in the beam is partitioned into two components (the primary and the fragment charge), it can be seen (Fig. 5) that the primary current is exponentially decreased as was the primary fluence.

If the number of particles in the beam is multiplied by the stopping power of particles (Eq. 1) then one obtains the dose as a funtion of penetration distance (Fig. 6). The experimental Bragg curve (points) includes the contribution of both the primary ions and the fragment particles which are produced in the nuclear collisions between the incident projectiles and the nuclei of the absorbers. The primary dose contribution is obtained from the number of surviving primary ions and their energy loss in the absorber. The major uncertainty in the result is from the number of primary ions in the beam. This can be measured with a particle telescope or any other particle detector which can distinguish the primary ions from the secondary ions.

The secondary dose contribution, which starts at zero and monotonically increased to a broad maximum near the Bragg peak and then decreases, is calculated in the same manner as the primary dose but it is the sum of the Bragg curve of the most probable charged fragments.

The secondary heavy charged particles in the beam are produced in nuclear interactions of the primary ions and the absorbing nuclei. Both nuclei may fragment in the collision. If the primary particle fragments, the fragments formed generally continue in the same direction and with the same velocity as the incoming ion [17]. The types of heavy charged particles that are produced can be any of the neotron deficient isotopes of the primary ion or isotopes of any lighter element with a mass less

than that of the incoming projectile. That is for a neon-20 projectile, the expected fragments would be isotopes of elements with Z = 1 to 9 with A≤20 or isotopes with Z=10 and A < 20. Generally the secondaries will have longer ranges than the primaries, however there will be some secondaries which will have a shorter ranges, (i.e., neutron deficient isotopes of the primary ion). In the calculations the energy per nucleon of each fragment is taken to be equal to that of the primary particle at the point of the collision. The contribution of each fragment to the dose is determined by the production probability. At a point near the Bragg peak the secondary dose approaches the primary dose.

Figure 7 shows permissible energy and energy loss values that can be expected for the most probably charged particles in the beam at a point a few centimeters before the Bragg peak. The energy per nucleon scale is useful because all particles with the same energy per nucleon will have the same velocity. Particles with nuclear charges of 1 to 10 are shown. The lighter fragments are distributed from some high energy/nucleon down to the energy/nucleon of the primary ions. For each element, this energy is a clue to the origin of the fragment. When produced the fragments, in general, will have the same energy per nucleon as the primary ions. Those with the lowest energy are usually closest to their point of origin; higher energies are associated with a greater distance to their origin. This relationship can be inverted for some neutron deficient isotopes becue of the range and energy loss relationships. Neutron deficient neon isotopes appear on the plot as the lower energy and higher rate of energy loss ions. If the data is presented as the rate of energy loss vs. total kinetic energy (Fig. 8) the plot takes on a different appearance and the isotopes of the different elements can be appreicated.

While the previous two figures do not give the relative probability of having a given particle with a specified energy, figure 9 shows the probability of having a particle with a specified average rate energy loss. Of more interest may be the number of particles with rates of energy loss below a given value (Fig. 10) or how the dose contribution varies with the average rate of energy loss (Fig. 11). Table 1 summarizes this data.

4. Discussion

The dose to a small mass of tissue can be calculated if all the particles passing through the small mass are known (Eq. 1). Therefore it is desirable to identify all the particles in the beams. This is a formidable job considering the number of different ion beams and energies involved.

In practice, the dose is usually obtained from a measurement with an ionization chamber located within a phantom. Ideally if the phantom ionization chamber and ionization chamber gas are tissue equivalent (TE) no corrections would be required to convert from the ionization chamber dose to the tissue dose.

Water, polystyrene or perspex are commonly substituted for a TE phantom. The relative dose and particle range in the phantom materials can be scaled by the relative electron densities [18]. For these ion beams, the carbon to oxygen ratio in the TE material is not as critical to the dosimetry as it is with neutron and pion beams. If a TE ionization chamber is used not with TE gas but with air as the filling gas, the required correction is determined from:

1) the change in the mass of the filling gas (ratio of densities is sufficient because the volume is the same),
2) the relative mass stopping powers of the two gases (these two items determine the energy lost in the gases), and
3) the ratio of the average energy expended to make an ion pair (w).

The mass (or volume) of the gas is determined by a calibration of the ionization chamber in a cobalt-60 beam.

The relative mass stopping power of gas to tissue can be determined from tabulated range-energy data. The stopping of the various materials for particles above a few MeV is assumed to be accurate to better than a few percent and the relative stopping power should have even higher accuracy.

The energy to make an ion pair (w) in the gas is taken to be the same as for a higher energy electron to make an ion pair [19]. Since the change in w occurs primarily at low velocities (< 2 MeV/u), it is relative unimportant for these heavy-charged particle beams at most depths of penetration. At the Bragg peak, a correction to w might be appropriate

The large accelerators that produce these heavy charged-particle beams are all pulsed machines. Pulse to pulse variations is shape and intensity are common. Corrections need to be considered for recombination in the ionization chambers [20]. Ideally any correction necessary should be applied on a per pulse basis because of the pulse shape variations normally encountered.

The determination of a heavy charged-particle absorbed dose, based upon an ionization measurement, may have an uncertainty as great as 10 percent. The large uncertainty is mainly from lack of information on:

1) the beam composition at various depths in the absorbing material,
2) the energy to make an ion pair for each particle passing through the ionization chamber,
3) the stopping power ratios of the different materials for the various particles,
4) and corrections for recombination of the ions produced in densely ionized tracks by the pulsed beams.

This beam model is used to supplement the experimental determination of the beam composition. Because of the uncertainties in the conversion factors the charged particle beam dosimetry task group of the American Association of Physicist in Medicine (1) recommends that the ionization chamber be calibrated with a TE calorimeter [21].

Table 1

Relative particle abundance and contribution to absorbed dose 4.1 cm upstream of the Bragg peak of a 557 MeV/u neon ion beam.

PARTICLE	PERCENT OF TOTAL PARTICLES	PERCENT CONTRIBUTION TO DOSE
protons	45	1.6
proton plus helium	65	3.1
$1 <= Z => 9$	85	40
$Z = 10$	15	60

(1) Draft protocol for charged particle beam dosimetry, being prepared by Task Group No. 20 of the American Association of Physicist in Medicine.

FIG. 1. Bragg curves of helium, carbon, neon and argon ion beams in water [5].

FIG. 2. Bragg curve of a 400 MeV/u neon ion beam and a range modulated dose distribution of the same beam in water [5].

FIG. 3. Energy of primary ions relative to the depth of penetration in a water medium.

FIG. 4. Number of primary, fragment and total particles relative to the depth of penetration.

FIG. 5. Beam current relative to the depth of penetration.

FIG. 6. Bragg curve of a neon ion beam. Also shown are the contributions of the primary ions and of the fragment particles.

FIG. 7. Range of allowable rate energy loss and energy per nucleon for charged particles expected 4.1 cm upstream of the Bragg peak. Each curve represents particles of a single element with an atomic number between and including 1 and 10.

FIG. 8. Range of allowable rate of energy loss and energy for charged particles expected 4.1 cm upstream of the Bragg peak.

FIG. 9. Fluence relative to the rate of energy loss 4.1 cm upstream of the Bragg peak.

FIG. 10. Cumulative fluence relative to the rate of energy loss 4.1 cm upstream of the Bragg peak.

FIG. 11. Cumulation dose relative to the rate of energy loss 4.1 cm upstream of the Bragg peak.

References

[1] ROESCH, W. C. and ATIX, F. H., "Basic concepts of dosimetry." In: Radiation Dosimetry Vol I 2nd ed., (Attix, F.H. and Roesch, W.C, Eds.), Academic Press, New York (1968).

[2] RAJU, M. R., LYMAN, J. T., BRUSTAD, T. and TOBIAS, C. A., "Heavy-charged particle beams." In: Radiation Dosimetry Vol III 2nd Ed., (Attix, F. H., Roesch, W. C., and Tochilin, E., Eds.), Academic Press, New York (1969).

[3] TODD, P.W., LYMAN, J. T., ARMER, R., SKARSGARD, L. D. and DEERING, R. A., Dosimetry and apparatus for heavy ion irradiation of mammalian cells in vitro. Radiat. Res. 34:1-23 (1970).

[4] SCHIMMERLING, W., VOSBURGH, K. G., TODD, P. W. and APPLEBY, A., Apparatus and dosimetry for high-energy heavy-ion beam irradiations. Radiat. Res. 65:389-413 (1976).

[5] LYMAN, J. T. and HOWARD, J., Dosimetry and Instrumentation for Helium and Heavy Ions. Int. J. Radiat. Oncol. Biol. Phys. 3:81-85 (1977).

[6] ACETO, H., JOLLY, R. K. and BUCKLE, D., Biophysical aspects of the Space Radiation Effects Laboratory (SREL) 710-MeV helium ion beam: Physical measurements and dosimetry. Radiat. Res. 77:5-20 (1979).

[7] LARSSON, B., "Dosimetry and radiobiology of protons as applied to cancer therapy and neurosurgery." Gustaf Werner Institute Report, GWI R 1/79 (1979).

[8] VERHEY, L. J., KOEHLER, A. M., MCDONALD, J. C., GOITEIN, M., MA, I., SCHNEIDER, R. J., and WAGNER, M., The determination of absorbed dose in a proton beam for purposes of charged-particle radiation theapy. Radiat. Res. 79:34-54 (1979).

[9] LITTON, G., LYMAN, J. AND TOBIAS, C., "Penetration of high-energy heavy ions with the inclusion of coulomb, nuclear and other stochastic processes," Lawrence Berkeley Laboratory Report UCRL-17392 rev., (1968).

[10] LYMAN, J. T. "Computer modeling of heavy charged-particle beams." Proceedings, International Workshop on Pion and Heavy Ion Radiotherapy: Pre-clinical and Clinical Studies, Vancouver,July, 1981 (to be published).

[11] WILSON, R. R., Radiological use of fast protons. Radiol. 47:487-491 (1946).

[12] CHATTERJEE, A., TOBIAS, C. A. and LYMAN, J. T., "Nuclear fragmentation in therapeutic and diagnostic studies with heavy ions." In: Spallation Nuclear Reactions and their Applications (Shen and Merker, Eds.), D. Reidel, Boston 161-191 (1976).

[13] SILBERBERG, R. and TSAO, C. H, Partial cross-sections in high-energy nuclear reactions, and astrophysical applications. I. Targets with $Z \leq 28$. Astrophys. J. Suppl. 25:315-333 (1973).

[14] KARLSSON, B. G., Methoden zur Berechnung und Erzielung einiger fur die Tiefentherapie mit hochenergitischen Protonen gunstiger Dosisverteilunger. Strahlentherapie 124:481-492 (1964).

[15] KOEHLER, A. M., SCHNEIDER, R. J. and SISTERSON, J. M. Range modulators for protons and heavy ions. Nucl. Inst. Meth. 131:437-440 (1975).

[16] AHLEN, S. P., Theoretical and experimental aspects of the energy loss of relativistic heavily ionizing particles. Rev. Mod. Phys. 52:121-173 (1980).

[17] Greiner, D. E., Lindstrom, P. J., Heckman, H. H., Cork, B., and Bieser, F. S., Momentum distributions of isotopes produced by fragmentation of relativistic ^{12}C and ^{16}O projectiles. Phys. Rev. Lett. 35:152-155 (1975).

[18] GOODMAN, L. J. and COLVETT, R. D., Biophysical studies with high-energy argon ions. 1. Depth dose measurements in tissue-equivalent liquid and in water. Radiat. Res. 70:455-468 (1977).

[19] ICRU. "Average energy required to produce an ion pair." ICRU Report 31, Washington (1979).

[20] BOAG, J. W., "Ionization chambers." In: Radiation Dosimetry Vol II 2nd ed., (Attix, F. H. and Roesch, W. C., Eds.), Academic Press, New York (1966).

[21] MCDONALD, J. C., LAUGHLIN, J. S. and FREEMAN, R. E., Portable tissue equivalent calorimeter. Med. Phys. 3:80-85 (1976).

This work was supported by the U.S. Department of Energy under Contract No. DE-AC03-76SF00098.

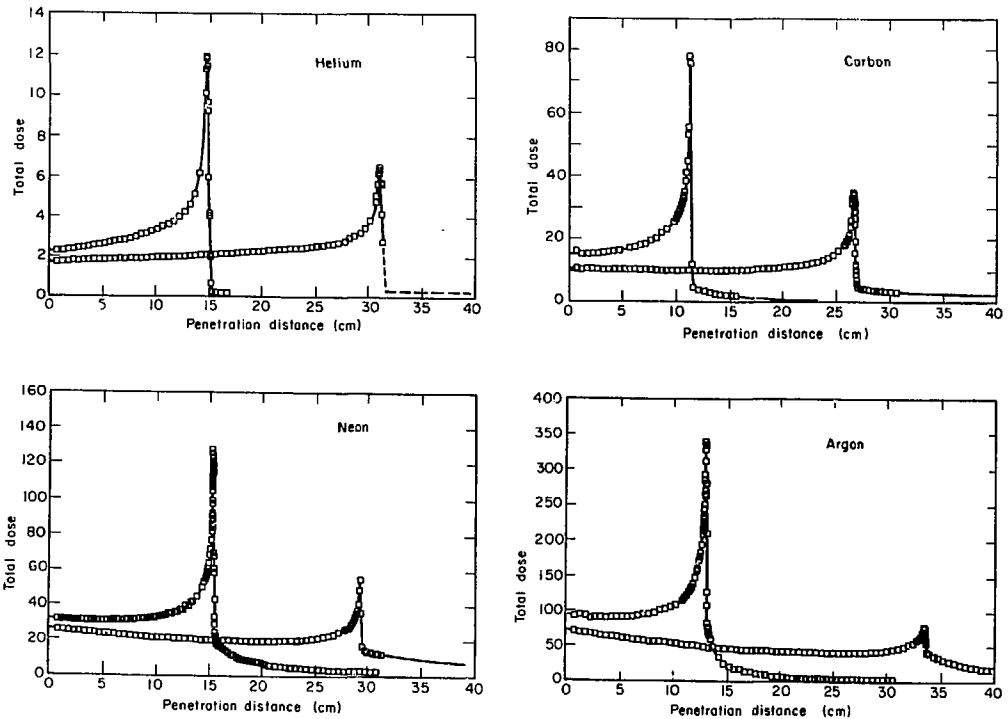

Figure 1

XBL768-9226

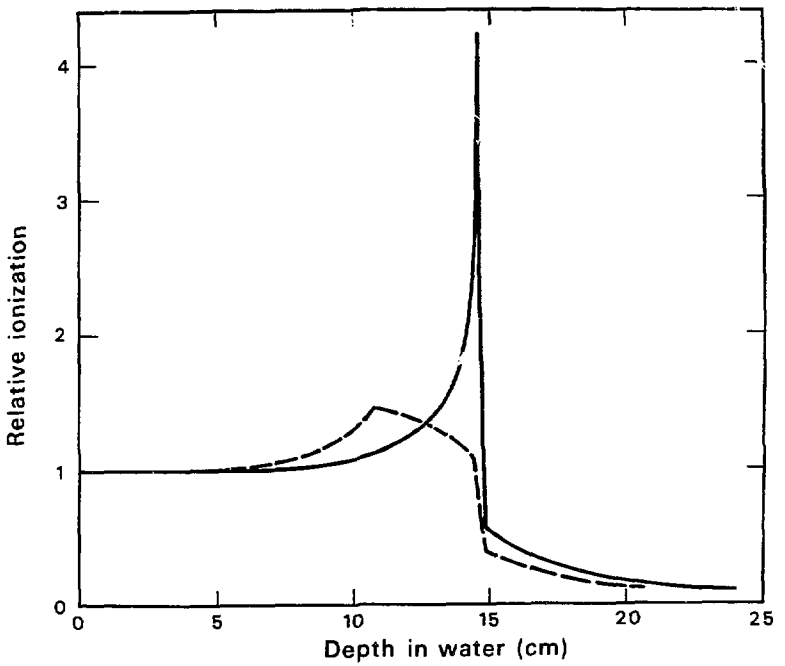
Relative ionization
0
1
2
3
4
0
5
10
15
20
25
Depth in water (cm)
XBL755-4910

Figure 2

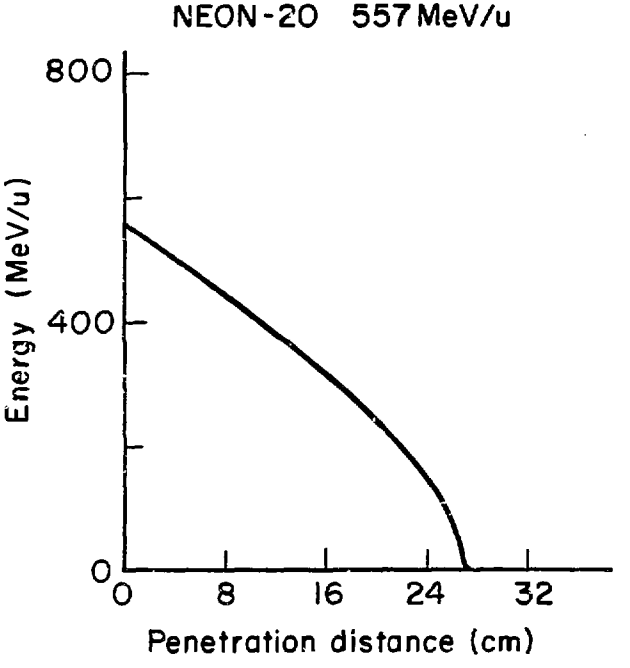

Figure 3

XBL821-3527

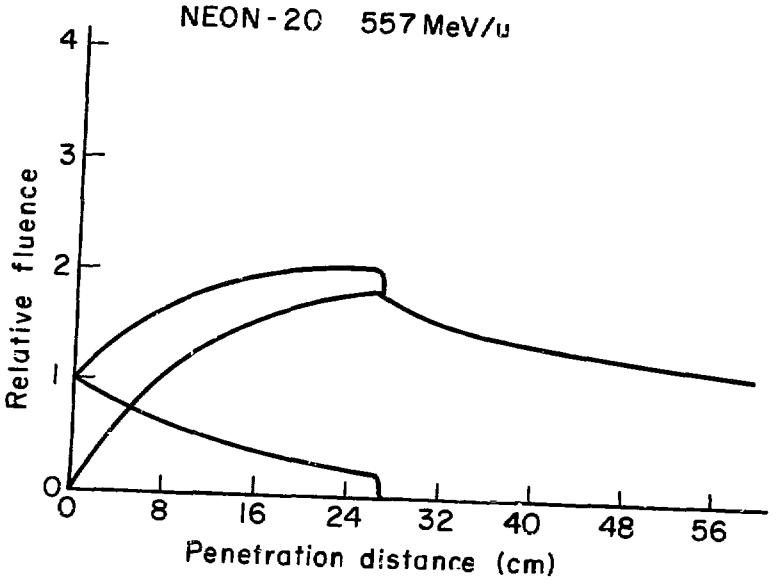

Figure 4

XBL821-3519

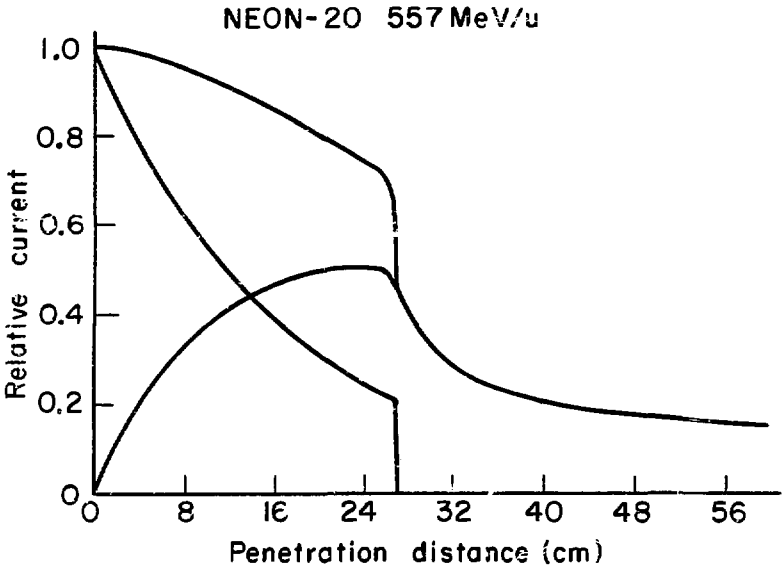

Figure 5

XBL821-3520

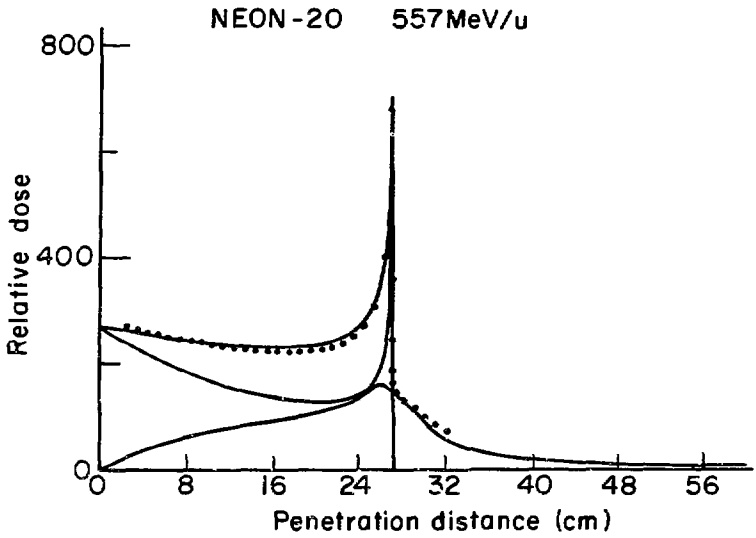

Figure 6

XBL 821-3521

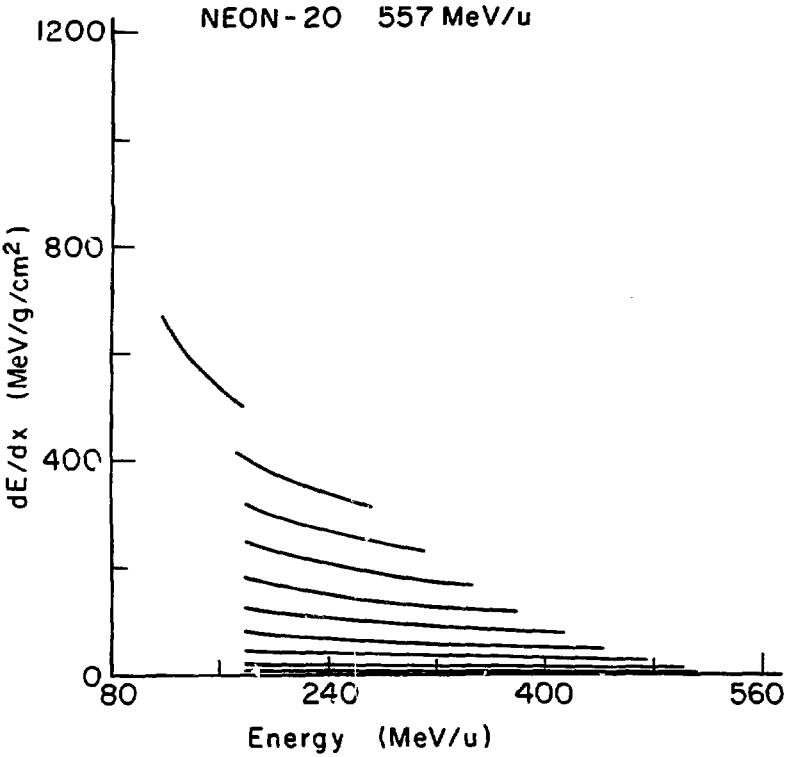

Figure 7

XBL821-3523

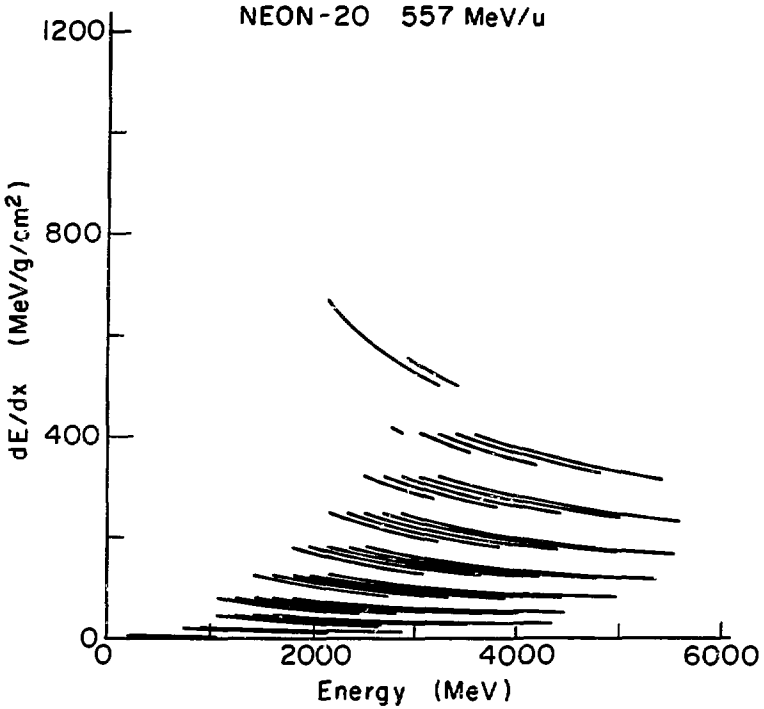

Figure 8

XBL821-3524

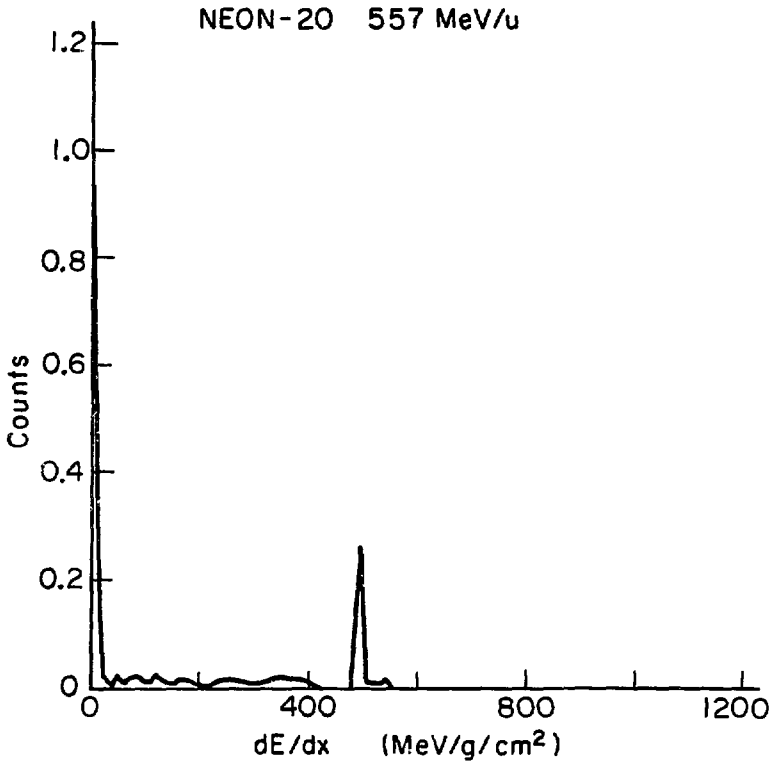

Figure 9

XBL 821-3525

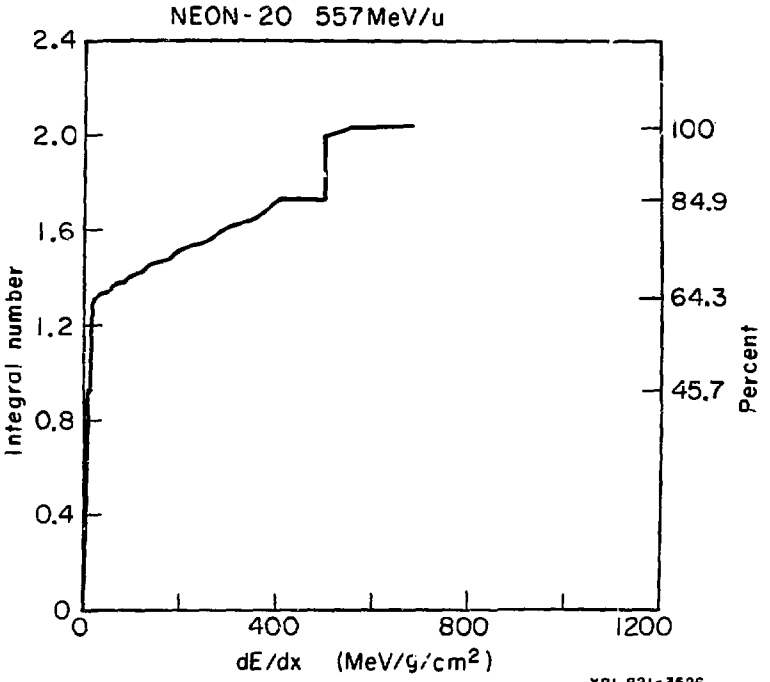
NEON-20 557MeV/u
2.4
2.0
1.6
1.2
0.8
0.4
0
Integral number
100
84.9
64.3
45.7
Percent
0
400
800
1200
dE/dx (MeV/g/cm²)
XBL 821-3526

Figure 10

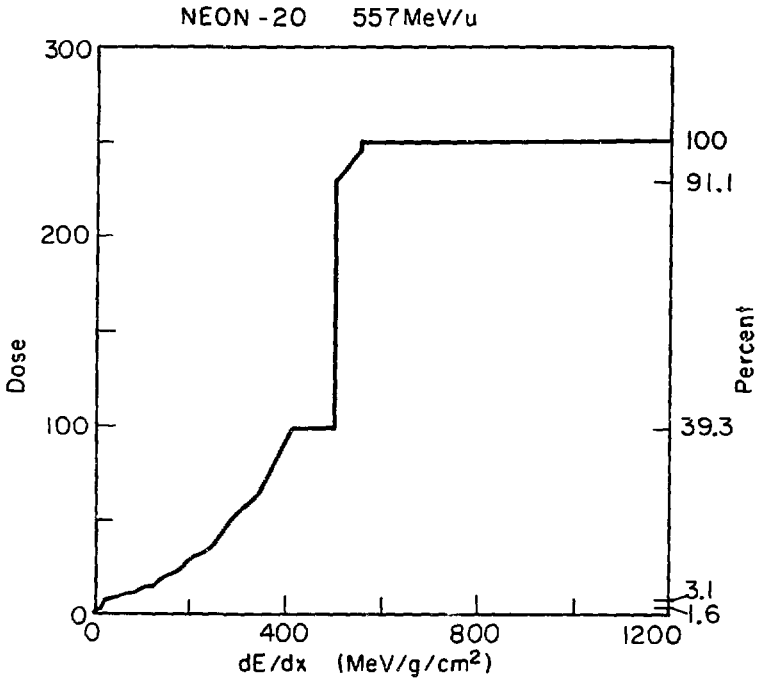

Figure 11

XBL821-3528

This report was done with support from the Department of Energy. Any conclusions or opinions expressed in this report represent solely those of the author(s) and not necessarily those of The Regents of the University of California, the Lawrence Berkeley Laboratory or the Department of Energy.

Reference to a company or product name does not imply approval or recommendation of the product by the University of California or the U.S. Department of Energy to the exclusion of others that may be suitable.